Journal of Power Sources 185 (2008) 1408–1414

Contents lists available at ScienceDirect

Journal of Power Sources

journal homepage: www.elsevier.com/locate/jpowsour

Preparation of $Li(Ni_{1/3}Co_{1/3}Mn_{1/3})O_2$ by spherical $Ni_{1/3}Mn_{1/3}Co_{1/3}OOH$ at a low temperature

Zhaorong Chang[a,*], Zhongjun Chen[a], Feng Wu[b], Hongwei Tang[a], Zhihong Zhu[a], Xiao Zi Yuan[c], Haijiang Wang[c]

[a] College of Chemistry and Environmental Science, Henan Normal University, Jianshe Road No. 46, Xinxiang 453007, PR China
[b] College of Chemical Engineering and Environment, Beijing Institute of Technology, Beijing 100080, PR China
[c] Institute for Fuel Cell Innovation, National Research Council of Canada, Vancouver, BC, Canada V6T 1W5

ARTICLE INFO

Article history:
Received 8 January 2008
Received in revised form 12 July 2008
Accepted 18 July 2008
Available online 25 July 2008

Keywords:
$Li(Ni_{1/3}Co_{1/3}Mn_{1/3})O_2$
Low temperature
$Ni_{1/3}Mn_{1/3}Co_{1/3}OOH$
Cathode material

ABSTRACT

Spherical $Li(Ni_{1/3}Co_{1/3}Mn_{1/3})O_2$ with a layered structure has been successfully prepared using the spherical precursor $Ni_{1/3}Mn_{1/3}Co_{1/3}OOH$ at temperature of 600 °C. This synthesis temperature is remarkably lower than those of the spherical $Li(Ni_{1/3}Co_{1/3}Mn_{1/3})O_2$ powders synthesized using $Ni_{1/3}Mn_{1/3}Co_{1/3}(OH)_2$ or $Ni_{1/3}Mn_{1/3}Co_{1/3}CO_3$. The compounds were characterized by X-ray diffraction (XRD), and scanning electron microscopy (SEM). XRD analysis shows that the $Ni_{1/3}Mn_{1/3}Co_{1/3}OOH$ powder has a P3 structure and the $Ni_{1/3}Mn_{1/3}Co_{1/3}(OH)_2$ powder has a T1 structure. Charge and discharge tests show that the $Li(Ni_{1/3}Co_{1/3}Mn_{1/3})O_2$ cathode prepared at 600 °C for 24 h has an initial discharge capacity as high as 148 mAh g^{-1}. The synthesized powder shows a reversible capacity of 142 mAh g^{-1} a specific current of 0.2C rate in the range of 3.0 V to 4.3 V up to 50 cycles with no noticeable capacity-fading.

1. Introduction

$LiCoO_2$ has been used as a major cathode material for lithium-ion batteries (LIBs) since it was first introduced by Sony Corporation, as it is easy to prepare and has good recharge ability even when the batteries are operated at very high rate [1]. However, the drawbacks of $LiCoO_2$, such as its toxicity and high cost, have intensified efforts to find an alternative cathode material for high-energy applications. The practical capacity of cathode material for LIBs has gradually been increased to meet the requirements of high-power and high-energy applications [2–4]. Recently, the mixed oxide $Li(Ni_{1/3}Co_{1/3}Mn_{1/3})O_2$ has been receiving increased attention as an alternative 4 V-cathode material for rechargeable LIBs due to its high capacity and stable structure [5–14]. Unfortunately, this compound is difficult to prepare using traditional solid state or solution methods. Various synthesis methods, such as hydroxide [15] and carbonate co-precipitation [16], sol–gel [17] and molten salt [18], have been employed in order to obtain superior electrode performance. Progress has been made in synthesizing powders to improve electrochemical performance, but the methods used normally require harsh synthesizing conditions. For example, $Li(Ni_{1/3}Co_{1/3}Mn_{1/3})O_2$ powders are usually synthesized at high temperatures between 900 °C and 1100 °C under long sintering time. It is obvious that high-temperature fabrication processes will lead to high capital outlays for equipment, along with significant energy costs during manufacturing. Therefore, it is necessary to search for a simpler method to synthesize $Li(Ni_{1/3}Co_{1/3}Mn_{1/3})O_2$ cathode material with improved volumetric energy density before the material can be used in practical cells.

It is well known that the physical properties of the cathode material, such as its morphology, particle-size distribution, tap-density and specific surface area, are very important for its use in a practical LIB. Therefore, a great deal of effort has been made to produce spherical $Li(Ni_{1/3}Co_{1/3}Mn_{1/3})O_2$. For example, hydroxide and carbonate co-precipitation have been employed using $Ni_{1/3}Mn_{1/3}Co_{1/3}(OH)_2$ or $Ni_{1/3}Mn_{1/3}Co_{1/3}CO_3$ to obtain a spherical product [15,16]. However, little attention has been paid to synthesizing spherical $Li(Ni_{1/3}Co_{1/3}Mn_{1/3})O_2$ powders using higher valences $Ni_{1/3}Mn_{1/3}Co_{1/3}OOH$.

In this paper, spherical powders of $Li(Ni_{1/3}Co_{1/3}Mn_{1/3})O_2$ were prepared using spherical $Ni_{1/3}Mn_{1/3}Co_{1/3}OOH$. The novelty of this paper is not the synthesis of the spherical $Li(Ni_{1/3}Mn_{1/3}Co_{1/3})O_2$ but the approaches of replacing the precursor of spherical $Ni_{1/3}Co_{1/3}Mn_{1/3}(OH)_2$ by $Ni_{1/3}Co_{1/3}Mn_{1/3}OOH$ at a relatively low temperature. In the literature, the synthesis temperature is generally above 900 °C when $Ni_{1/3}Co_{1/3}Mn_{1/3}(OH)_2$ is used as a

* Corresponding author. Tel.: +86 373 3326544; fax: +86 373 3326544.
E-mail address: czr_56@163.com (Z. Chang).

0378-7753/$ – see front matter © 2008 Elsevier B.V. All rights reserved.
doi:10.1016/j.jpowsour.2008.07.039

precursor. To date, the synthesis of $Li(Ni_{1/3}Co_{1/3}Mn_{1/3})O_2$ using $Ni_{1/3}Mn_{1/3}Co_{1/3}OOH$ at such a low temperature and in an air atmosphere has not been reported. For the first time, we report the approaches of preparing spherical $Li(Ni_{1/3}Co_{1/3}Mn_{1/3})O_2$ using spherical $Ni_{1/3}Mn_{1/3}Co_{1/3}OOH$ and $LiNO_3$ by sintering at 600 °C in air. The procedures are described in terms of crystallinity and particle sizes. The electrochemical performance of a $Li/Li(Ni_{1/3}Co_{1/3}Mn_{1/3})O_2$ cell was also investigated.

2. Experimental

The spherical precursor $Ni_{1/3}Co_{1/3}Mn_{1/3}OOH$ was obtained as described below. Stoichiometric amounts of $NiSO_4{\cdot}6H_2O$, $CoSO_4{\cdot}7H_2O$, and $MnSO_4{\cdot}H_2O$ were dissolved together in distilled water (transition metal ratio of Ni:Co:Mn = 1:1:1) and the concentration of the total metal sulfate was 2 mol l^{-1}. The aqueous solution was precipitated by adding a NaOH solution (aq.) of 2 mol l^{-1} and a certain amount of NH_4OH solution (aq.) under an argon atmosphere, stirring continuously. The solution was maintained at 50 °C for 20 h and the pH value was controlled at approximately 10–11. Then, the obtained spherical precursor of $Ni_{1/3}Mn_{1/3}Co_{1/3}(OH)_2$ was oxidized by adding a given amount of H_2O_2 in 4 mol l^{-1} KOH solution. The desired spherical precursor was obtained after filtering, washing and drying at 50 °C for 2 h.

Synthesis of $Li(Ni_{1/3}Co_{1/3}Mn_{1/3})O_2$ was carried out using a solid state reaction. $LiNO_3$ with a melting point of 264 °C was used as the lithium salt. The obtained precursor powder $Ni_{1/3}Co_{1/3}Mn_{1/3}OOH$ was mixed with 1% excess $LiNO_3$. The excess amount of Li salts was used to compensate for possible Li loss during calcination. The mixtures were initially heated to 300 °C for 3 h, and subsequently calcined at 600 °C for 24 h in air. The heating rate was fixed at 120 °C h^{-1} for all the temperature settings. After heating, the resulting powders were cooled to ambient temperature.

Thermogravimetric/differential thermal analyzer (TG/DSC) analysis was carried out on a simultaneous thermal analysis apparatus NETZSCH STA409 PC/PG (Netzsch, Germany) to determine the sintering temperature. The mixture was heated from room temperature to 900 °C at a heating rate of 4 °C min^{-1}. The measurement was performed in nitrogen flow using α-Al_2O_3 as the reference material.

To investigate the crystal structure, the obtained powders were analyzed by X-ray diffraction (XRD) using a D8 X diffractometer (Germany, Bruker) employing Cu Kα radiation. The scan data were collected in the 2θ range of 10–80°. The step size was 0.026° with a counting time of 3 s. The morphology of the synthesized powder was investigated by a field emission scanning electron microscope, SEM-6701F (Japan, JOEL). X-ray photoelectron spectroscopy (XPS) of the synthesized powder was performed with a VG ESCALab 220I-XL spectrometer (UK, VG Scientific) with a Mono Al X-ray source (1486.6 eV). The collected spectra were analyzed using XPS-PEAK41 fitting software. The energy scale was adjusted based on the graphite peak in the C 1s spectrum at 284.6 eV.

Slurries containing 85 wt.% active material, 5 wt.% polyvinylidene fluoride dissolved in *n*-methyl-2-pyrrolidinone and 10 wt.% acetylene black were spread evenly on a piece of aluminium foil. The sheet was subsequently dried at 120 °C for 10 h and was then cut into pieces for cathodes. One mole per liter of $LiPF_6$ in ethylene carbonate and diethyl carbonate (1:1, v/v) was used as the electrolyte solution. Coin cells (CR2025) were assembled with metallic Li as the counter electrode and Celgard 2400 as the separator in an Ar-filled glove box. The cells were cycled between 3.0 V and 4.3 V versus Li/Li^+ galvanostatically (*C*/5 rate) on a Land CT2001A battery tester (Wuhan Jinnuo Electronics Co. Ltd., China) at room temperature.

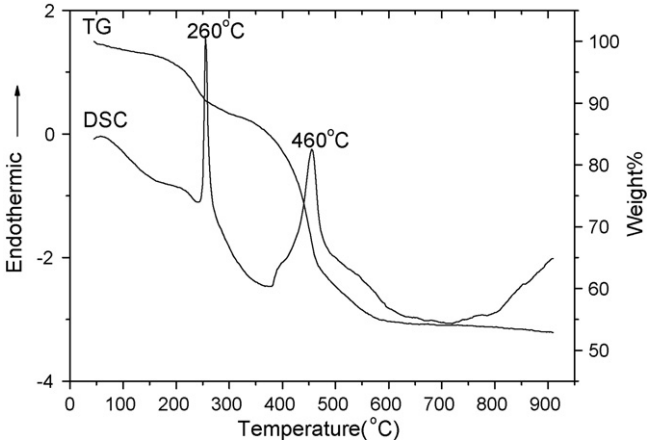

Fig. 1. TG/DSC analysis for $LiNO_3$ and precursor.

3. Results and discussion

3.1. TG/DSC analysis

In order to optimize the temperature range for the reaction, TG/DSC analysis was carried out. The results are plotted in Fig. 1, which shows the TG/DSC curves of the mixture of the precursor and the lithium salt $LiNO_3$. It can be seen that there are two weight losses and two visible endothermal peaks in the temperature range of 160–600 °C. The first endothermal peak is observed approximately at 260 °C from the DSC curve, accompanied without notable weight loss seen from the corresponding TG curve. This represents that the first endothermal peak is caused by the melting process of $LiNO_3$ (the melting point is 264 °C). There is a slight weight loss between 140 °C and 250 °C, which is attributed to the evaporation of water. The second obvious endothermic peak at 460 °C shows the decomposition of $LiNO_3$, which continues up to 600 °C and is marked by a mass weight loss from 400 °C to 570 °C in the TG curve. When the temperature is higher than 600 °C, the TG curve indicates that the weight remains constant. We may conclude that the stable phase of $Li(Ni_{1/3}Mn_{1/3}Co_{1/3})O_2$ could form at 600 °C. Based on this analysis, it was reasonable to synthesize the compound of $LiNi_{1/3}Mn_{1/3}Co_{1/3}O_2$ by two steps. First, the mixtures of the precursor and $LiNO_3$ were calcined at 300 °C for 3 h in order to thoroughly soak the molten salt in the precursor and, at the same time, prevent the evaporation of lithium salt at high temperature. They were then sintered at 600 °C to synthesize the desired powder.

3.2. XRD and SEM analysis of the precursor

Fig. 2a and b shows the XRD spectra of the obtained $Ni_{1/3}Co_{1/3}Mn_{1/3}(OH)_2$ and $Ni_{1/3}Co_{1/3}Mn_{1/3}OOH$ powder. It can be observed from Fig. 2a that the spectra are almost the same as those of pure β-$Ni(OH)_2$ [19], which indicates that the valence of Ni, Co, and Mn is 2+. Based on Van der Ven et al.'s theory [19], it can be concluded that the crystal structure of $Ni_{1/3}Co_{1/3}Mn_{1/3}(OH)_2$ powder consists of close-packed oxygen planes with an ABAB oxygen stacking, which has the T1 stacking sequence. The metal atoms occupy octahedral sites between alternating oxygen layers, and the hydrogen atoms reside in the tetrahedral sites of the remaining layers between oxygen. As can be seen from Fig. 2b, the XRD spectra of $Ni_{1/3}Co_{1/3}Mn_{1/3}OOH$ powder are similar to those of pure β-NiOOH, which has a P3 host structure [19]. This host structure consists of an AABBCC oxygen stacking sequence, which favors the exchange between Li^+ and H^+ during the reaction of $Ni_{1/3}Co_{1/3}Mn_{1/3}OOH$ and $LiNiO_3$, and oxygen stacking shifts from

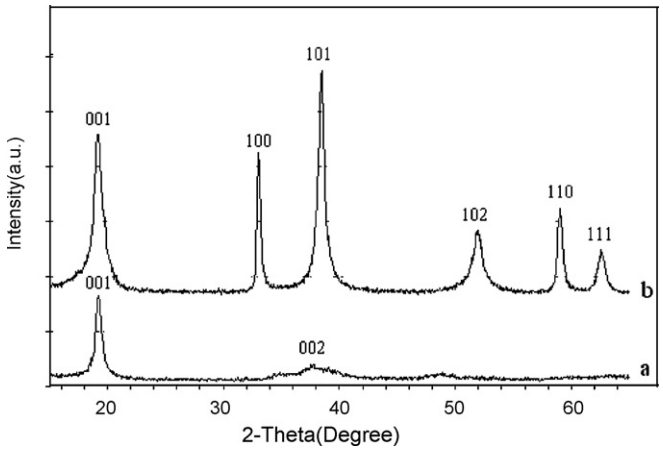

Fig. 2. XRD patterns of different precursor. (a) The $(Ni_{1/3}Co_{1/3}Mn_{1/3})OOH$ precursor.(b) The $Ni_{1/3}Co_{1/3}Mn_{1/3}(OH)_2$ precursor.

P3(AABBCC) to O3(ABCABC) without breaking any O–TM bonds. Therefore, it is possible to synthesize $Li(Ni_{1/3}Mn_{1/3}Co_{1/3})O_2$ powders at low temperature by the precursor of $Ni_{1/3}Co_{1/3}Mn_{1/3}OOH$. Furthermore, Van der Ven et al.'s calculations by the first-principle show that the P3 structure are more stable than T1 structure. The T1 structure is dynamically unstable, and easily transforms to P3 without an energy barrier, which corresponds with the experiment fact that the $Ni_{1/3}Co_{1/3}Mn_{1/3}(OH)_2$ is easy to be transformed to the $Ni_{1/3}Co_{1/3}Mn_{1/3}OOH$ powder in air.

Fig. 3a–c shows the morphology of the $Ni_{1/3}Co_{1/3}Mn_{1/3}OOH$ powders. The powders are composed of well-dispersed spherical particles. Each of the spherical particles is composed of a large number of sheet crystalline grains, and as shown in Fig. 3c, these sheet crystalline grains are slightly curved, intercrossed, and overlapped, resulting in a large number of pores. When the precursor is mixed with the lithium salt these pores help the molten lithium salt to soak into the interspaces and directly contact the crystalline grains. Thus, the Li^+ in the molten salt can easily diffuse throughout the particles, which accelerates the reaction of the $Li(Ni_{1/3}Co_{1/3}Mn_{1/3})O_2$ synthesis.

3.3. XPS analysis of the precursor

In order to confirm the oxidation state of the transition metal species in the synthesized materials of the precursor, XPS study was carried out. Fig. 4a–c shows the XPS binding energy (BE) of Mn $2p_{3/2}$, Ni $2p_{3/2}$, and Co $2p_{3/2}$, respectively, of the precursor. In the Ni XPS spectra, a characteristic satellite peak is noted in addition

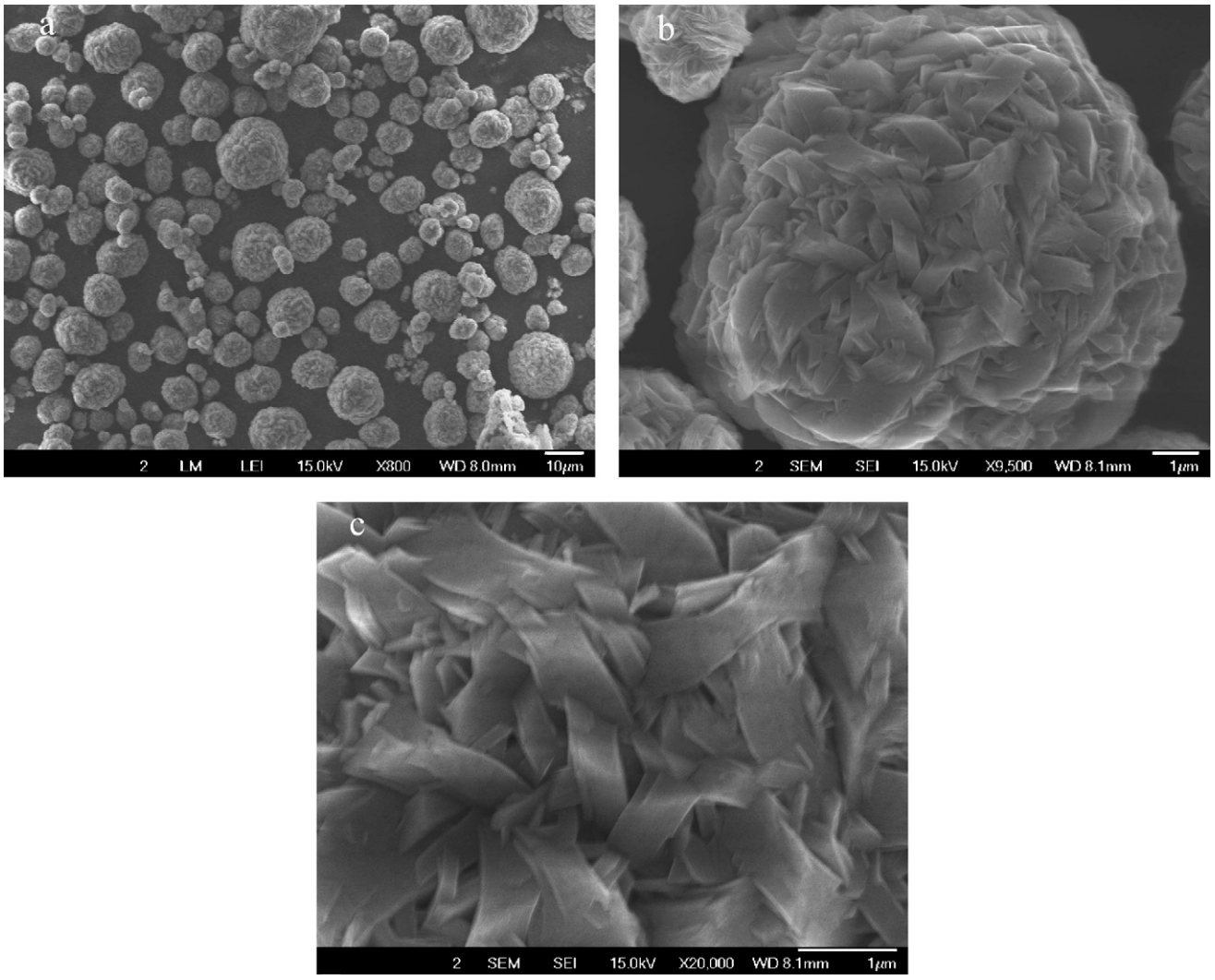

Fig. 3. SEM images of the $(Ni_{1/3}Co_{1/3}Mn_{1/3})OOH$ powder at different magnifications.

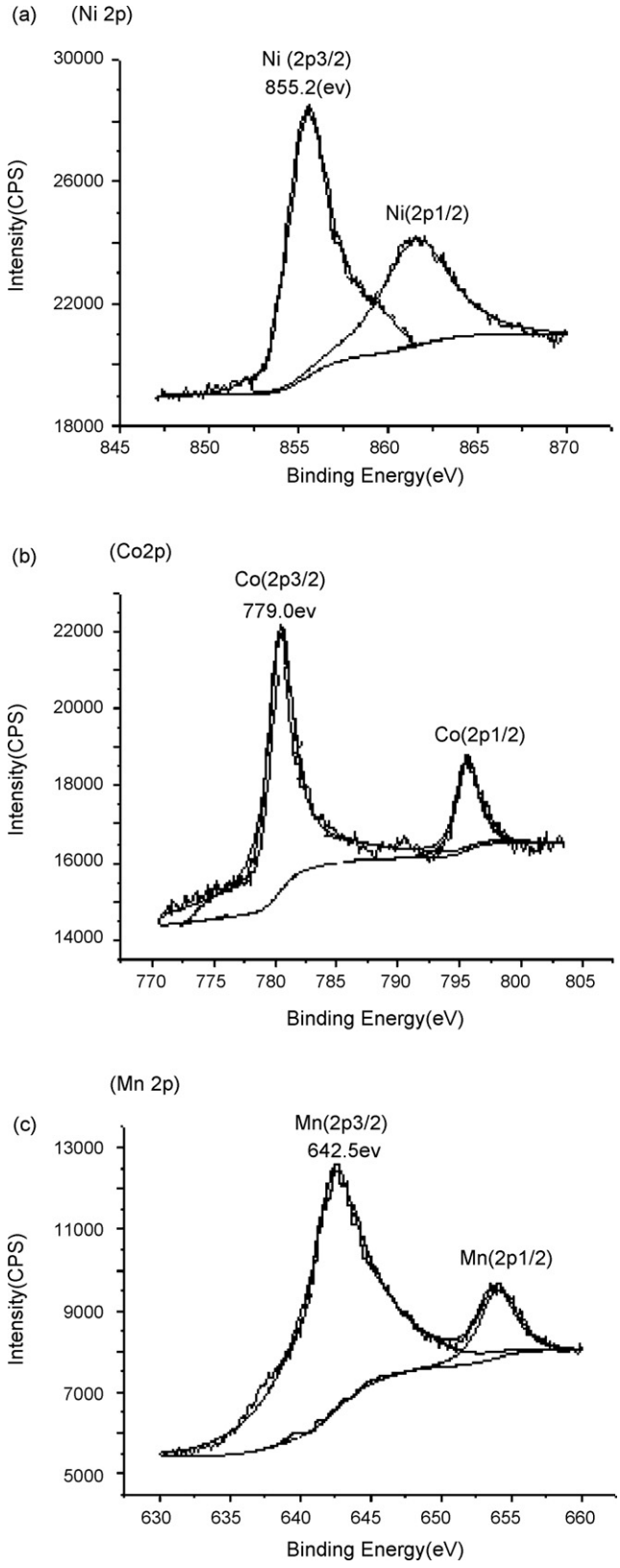

Fig. 4. XPS of (a) Ni_{2p}, (b) Co_{2p} and (c) Mn_{2p} of the synthesized precursor.

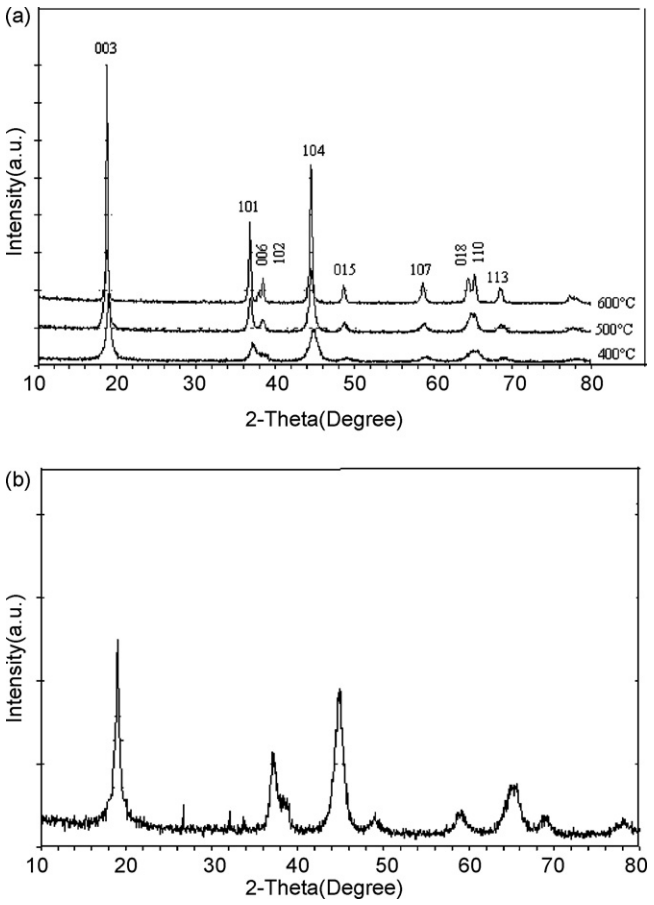

Fig. 5. XRD patterns of $Li(Ni_{1/3}Co_{1/3}Mn_{1/3})O_2$ samples sintered at different temperature by different precursor for 24 h. (a) The samples synthesized by $(Ni_{1/3}Co_{1/3}Mn_{1/3})OOH$ sintered at (400 °C, 500 °C and 600 °C) for 24 h. (b) The powders prepared by $Ni_{1/3}Co_{1/3}Mn_{1/3}(OH)_2$ sintered at 600 °C for 24 h.

to the $Ni(2p_{3/2})$ peak. Such a satellite peak was also observed in $Ni(OH)_2$ [20,21] and was explained as being due to multi-electron excitation (shake-up peaks). Curve fitting of the Ni $2p_{3/2}$ signals gives one nickel species. The peak with BE = 855.2 (Fig. 4a) agrees with those reported for $Ni(OH)_2$ [20,21]. As shown in Fig. 4b, the best fit for the $Co(2p_{3/2})$ spectrum gives two BE values. The major peak is at 779.0 eV and the minor one is at 780.4 eV. These values match well with the BE reported for CoOOH and $Co(OH)_2$ components [22,23]. Estimated from the area under the curve fitting, the ratio of CoOOH and $Co(OH)_2$ is 8:1. In Fig. 4c, the Mn 2p XPS spectrum consists of a Mn $2p_{3/2}$ XPS core line at 642.5 eV and a Mn $2p_{1/2}$ XPS line at 653.7 eV. The deconvolution of the $Mn(2p_{3/2})$ spectrum also gives two BEs for its best fit. Compared with the Mn $2p_{3/2}$ XPS core lines of MnOOH at 641.7 eV and MnO_2 at 642.5 eV [24], the major peak centered at 642.5 eV is MnO_2 and the minor one at 641.7 eV is MnOOH. Estimated from the area under the deconvoluted curve, the ratio of Mn^{4+} and Mn^{3+} is 9.2:1. It is obvious that the predominant valence of Mn in the precursor is 4^+ with a small amount of Mn^{3+}. In the present case, the prepared compound with Ni, Co and Mn ions are in 2^+, 3^+ and 4^+ oxidation states, respectively, and the average valence of the precursor is about 3^+. Based on the crystal field theory, the stabilities of Mn^{2+}, Co^{2+}, and Ni^{2+} are in the sequence of $Mn^{2+} < Co^{2+} < Ni^{2+}$ when spin octahedral complex ions with the same ligands are formed. This stability sequence has a significant influence on the existing state of the transition metal ions. From the d electron orbit point of view, the d electron configura-

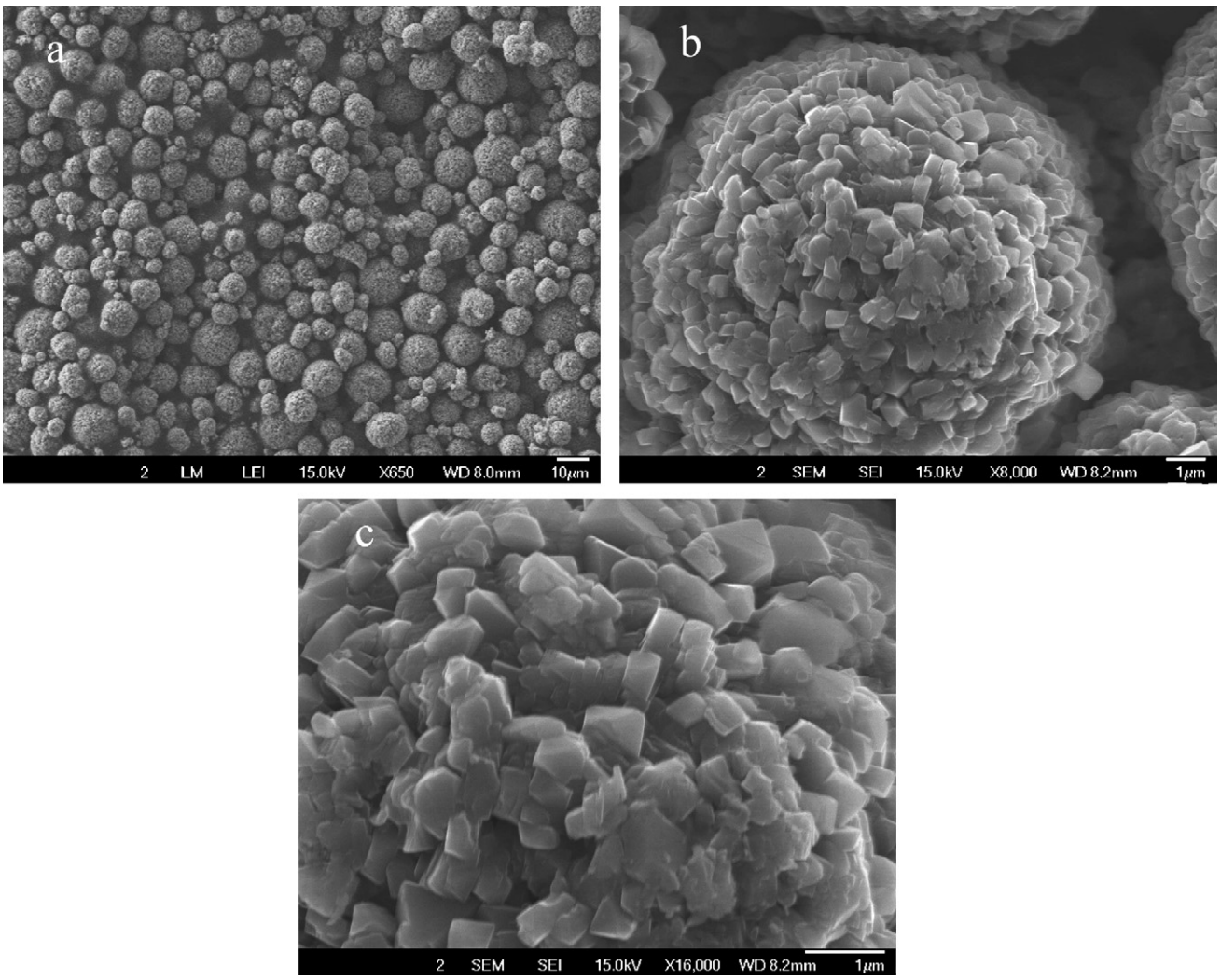

Fig. 6. SEM images of the $Li(Ni_{1/3}Co_{1/3}Mn_{1/3})O_2$ powder at different magnifications.

tions of Mn^{2+}, Co^{2+}, and Ni^{2+} are $t_{2g}^5e_g^0$, $t_{2g}^6e_g^1$, and $t_{2g}^6e_g^2$, respectively. It is known that the impair e_g electrons will result in an uneven occupancy of the electron orbit, further causing Jahn–Teller effect. Therefore, the changes of the structure and performance of the produced compounds are easy to occur. If the d electron structure of the cations could be changed to avoid the impair e_g electrons, lattice relaxation would be effectively restrained. Then a steady structure and performance of the compound would be achieved [25]. Based on this analysis, if the transition metal ions in the precursor were oxidized to a relatively steady state, for example, Mn^{2+} to Mn^{4+} ($t_{2g}^3e_g^0$), and Co^{2+} to Co^{3+} ($t_{2g}^6e_g^0$) (Ni^{2+} keeps its state of Ni^{2+} ($t_{2g}^6e_g^2$)), there would be no impair e_g electrons in the outer d electrons of the transition ions ($Co^{3+}|Ni^{2+}|Mn^{4+}$), avoiding the Jahn—Teller effect. Therefore, the structure and performance of the synthesized $Ni_{1/3}Co_{1/3}Mn_{1/3}OOH$ precursor would be relatively steady so that the single phase of $Li(Ni_{1/3}Co_{1/3}Mn_{1/3})O_2$ with a steady structure and performance could be obtained easily by $Ni_{1/3}Co_{1/3}Mn_{1/3}OOH$. In addition, as the valences or oxidation states of the metal ions in the precursor ($Ni_{1/3}Co_{1/3}Mn_{1/3}OOH$) are close to those in the product ($Li(Ni_{1/3}Co_{1/3}Mn_{1/3})O_2$), the dependence on the synthesis atmosphere and condition for oxidizing the metal ions is decreased. Thus, it is possible to synthesize the $Li(Ni_{1/3}Co_{1/3}Mn_{1/3})O_2$ cathode material for LIBs with layered structure and high crystallinity under relatively mild conditions, e.g., an air atmosphere, and a low temperature.

3.4. XRD analysis of the synthesized $Li(Ni_{1/3}Co_{1/3}Mn_{1/3})O_2$

Fig. 5a presents the XRD patterns for the samples prepared by the precursor of $Ni_{1/3}Co_{1/3}Mn_{1/3}OOH$ at calcination temperatures of 400, 500 and 600 °C for 24 h, respectively. The XRD patterns of all the materials can be indexed by a hexagonal α-$NaFeO_2$ structure (space group: $R\bar{3}m$), and no obvious impurity phases can be observed. As can be seen from Fig. 5a, the (0 0 3) and (1 0 1) peaks continuously shift to lower angles while the temperature increases, suggesting that Li ions intercalation results in the lattice expansion along *a*, *b*, *c* direction. Furthermore, it is found that the intensities of the diffraction peaks increase with increasing heat-treatment temperature. In the XRD patterns, an intensity ratio of the (0 0 3)/(1 0 4) peaks with a value lower than 1.2 has been recognized as a criterion for the existence of cation mixing in the powders [26]. In addition, the separation between (0 1 8)/(1 1 0) and (0 0 6)/(1 0 2) lines can be used to judge the structure arrangement order [27,28]. According to Fig. 5a, the intensity ratio of (0 0 3) and (1 0 4) peaks ($I_{003}/I_{104} = 1.8$) at 600 °C is higher than those at other temperatures. The (0 1 8) and (1 1 0) peaks and the

(0 0 6) and (1 0 2) lines are clearly split when the heating temperature is 600 °C. *R*-factor, defined as $(I_{006}+I_{102})/I_{101}=0.496$, indicates a high degree of crystallinity and a good hexagonal order. In other words, $Li(Ni_{1/3}Co_{1/3}Mn_{1/3})O_2$ powder can be synthesized by $Ni_{1/3}Co_{1/3}Mn_{1/3}OOH$ at a low temperature of 600 °C.

Fig. 5b shows the XRD patterns of the $Li(Ni_{1/3}Co_{1/3}Mn_{1/3})O_2$ cathode materials synthesized by the precursor of $Ni_{1/3}Co_{1/3}Mn_{1/3}(OH)_2$ at 600 °C for 24 h. It is clear that there are peaks caused by impurities at $2\theta=26°$, 32° and 34°, which indicates that pure $Li(Ni_{1/3}Co_{1/3}Mn_{1/3})O_2$ can not be obtained when mixing $Ni_{1/3}Co_{1/3}Mn_{1/3}(OH)_2$ and $LiNO_3$ at this temperature. In addition, The (0 1 8) and (1 1 0) peaks and the (0 0 6) and (1 0 2) lines are not split, which indicates that $Li(Ni_{1/3}Co_{1/3}Mn_{1/3})O_2$ powders can not be synthesized by $Ni_{1/3}Co_{1/3}Mn_{1/3}(OH)_2$ at a low temperature of 600 °C.

3.5. Morphology of the $Li(Ni_{1/3}Mn_{1/3}Co_{1/3})O_2$ powder

Fig. 6a–c shows the morphology of the synthesized $Li(Ni_{1/3}Co_{1/3}Mn_{1/3})O_2$ powders for the LIB cathode at different magnifications. From Fig. 6a, it is observed that the synthesized $Li(Ni_{1/3}Co_{1/3}Mn_{1/3})O_2$ powders maintain the precursor's spherical particles, ranging in size from 13 μm to 15 μm. The interfaces of the particles are clearly seen, and no aggregation is found. As shown in Fig. 6b and c, each of the spherical particles is made up of many crystalline grains. These granular particles are regularly polyhedron-shaped, ranging in size from 200 nm to 500 nm. The surface of the spherical particles is tidy and smooth, indicating the possibility of synthesizing $Li(Ni_{1/3}Co_{1/3}Mn_{1/3})O_2$ with high crystallinity and purity by the calcination of the mixture of the oxidized precursor and the lithium salt at a low temperature. This agrees with the results from XRD. Fig. 6c also shows that there are some interspaces among the granular crystalline grains of the spherical particle. When the $Li(Ni_{1/3}Co_{1/3}Mn_{1/3})O_2$ cathode material is used in LIBs, the liquid electrolyte can easily soak into the interspaces and directly contact the crystalline grains. Thus, the Li^+ in the liquid electrolyte can easily diffuse throughout the $Li(Ni_{1/3}Co_{1/3}Mn_{1/3})O_2$ particles, which helps the material to achieve good electrochemical performance.

3.6. Electrochemical properties

Fig. 7a shows the initial discharge curves for the $Li(Ni_{1/3}Co_{1/3}Mn_{1/3})O_2$ powders prepared by different precursors at 600 °C for 24 h. The electrode was cycled over the voltage range of 3.0–4.3 V at a constant current density of 0.2*C* (1*C* = 180 mAh g^{-1}) rate at 25 °C. The constant voltage (4.3 V) charge was applied to each cell until the current decreased to 1/10th of its initial value during the charging process. In the first cycle, the sample A prepared by $Ni_{1/3}Co_{1/3}Mn_{1/3}OOH$ delivered a reversible discharge capacity of 148 mAh g^{-1}, which was much higher than that of the powder (sample B) synthesized by the conventional $Ni_{1/3}Co_{1/3}Mn_{1/3}(OH)_2$ precursor (105 mAh g^{-1}). In order to determine the cyclability of the $Li(Ni_{1/3}Co_{1/3}Mn_{1/3})O_2$ cathode material at a 0.2*C* rate between 3 V and 4.3 V, $Li(Ni_{1/3}Co_{1/3}Mn_{1/3})O_2$ cathode of the two samples were tested for 50 cycles. Fig. 7b shows the results of the cycling test. The reversible capacity after 50 cycles is 142 mAh g^{-1} (96% of the first discharge capacity) for sample A. But the capacity retention at the 50th cycle is only 15 mAh g^{-1} for sample B. It is obvious that the cyclability of sample A at the same current density is much better than that of sample B. These results confirm that the cyclic performance of $LiNi_{1/3}Mn_{1/3}Co_{1/3}O_2$ synthesized by $Ni_{1/3}Co_{1/3}Mn_{1/3}OOH$ is superior to that of the $LiNi_{1/3}Mn_{1/3}Co_{1/3}O_2$ powders prepared by the conventional $Ni_{1/3}Co_{1/3}Mn_{1/3}(OH)_2$ precursor. The excellent cycling stability of sample A attributes to the uniform particle size and the highly ordered layered structure of the final $Li(Ni_{1/3}Co_{1/3}Mn_{1/3})O_2$ powder.

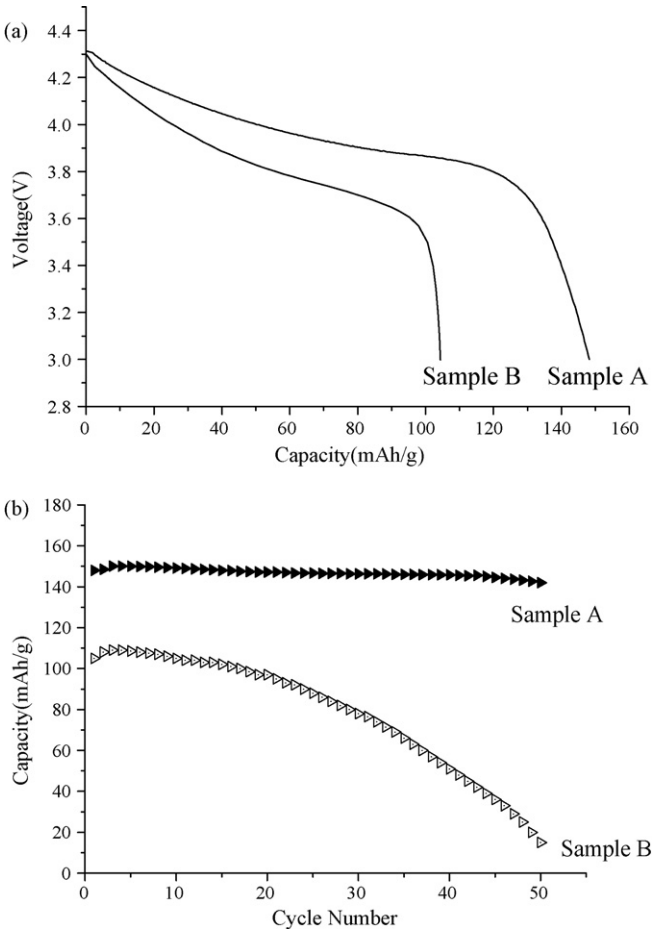

Fig. 7. The charge–discharge curves for $Li(Ni_{1/3}Co_{1/3}Mn_{1/3})O_2$ synthesized at 600 °C for 24 h. (a) The initial charge–discharge curves. (b) The $Li(Ni_{1/3}Co_{1/3}Mn_{1/3})O_2$ powder cyclic performance.

4. Conclusions

In this paper, spherical $Li(Ni_{1/3}Co_{1/3}Mn_{1/3})O_2$ with a layered structure has been successfully prepared by using the spherical precursor of $Ni_{1/3}Mn_{1/3}Co_{1/3}OOH$ at 600 °C for 24 h. Thus, the use of $Ni_{1/3}Mn_{1/3}Co_{1/3}OOH$ to synthesize $Li(Ni_{1/3}Mn_{1/3}Co_{1/3})O_2$ can avoid high-temperature fabrication processes, resulting in lower capital outlays for fabrication equipment and significant reductions in energy costs during the commercial powder manufacturing.

The morphologies of the $Li(Ni_{1/3}Mn_{1/3}Co_{1/3})O_2$ powders exhibit clearly hexagonal shapes together with homogeneous size distribution. The synthesized $Li(Ni_{1/3}Mn_{1/3}Co_{1/3})O_2$ has an excellent discharge capacity of 148 mAh g^{-1} (at 0.2*C*) in the first cycle with an excellent capacity retention rate of more than 96% after 50 cycles. Thus, to synthesize $Li(Ni_{1/3}Mn_{1/3}Co_{1/3})O_2$ by using the spherical precursor of $Ni_{1/3}Mn_{1/3}Co_{1/3}OOH$ is a promising method for rechargeable LIBs.

Acknowledgements

This work is financially supported by the Natural Science Foundation of China under approval No. 20671031.

References

[1] J.N. Reimers, J.R. Dahn, J. Electrochem. Soc. 139 (1992) 2091–2097.
[2] J.M. Kim, N. Kumagai, H.T. Chung, Electrochem. Solid State Lett. 9 (2006) A494–A498.
[3] C.H. Song, A.M. Stephan, S.K. Jeong, A.R. Kim, K.S. Nahm, Y.S. Lee, J.K. Kim, H.T. Chung, Mater. Res. Bull. 41 (2006) 1487–1495.
[4] H. Gabrisch, J.D. Wilcox, M.M. Doeff, Electrochem. Solid State Lett. 9 (2006) A360–A363.
[5] L. Zhang, X. Wang, T. Muta, D. Li, H. Noguchi, M. Yoshio, R. Ma, K. Takada, T. Sasaki, J. Power Sources 162 (2006) 629–635.
[6] W.S. Yoon, C.P. Grey, M. Balasubramanian, X.Q. Yang, D.A. Fischer, J. McBreen, Electrochem. Solid State Lett. 7 (2004) A53–A55.
[7] H.S. Kim, S.I. Kim, W.S. Kim, Electrochim. Acta 52 (2006) 1457–1461.
[8] S.H. Park, C.S. Yoon, S.G. Kang, H.S. Kim, S.I. Kim, S.I. Moon, Y.K. Sun, Eletctrochim. Acta 49 (2004) 557–563.
[9] D.C. Li, T. Muta, L.Q. Zhang, M. Yoshio, H. Noguchi, J. Power Sources 132 (2004) 150–155.
[10] Y.M. Todorov, K. Numata, Electrochim. Acta 50 (2004) 495–499.
[11] S.H. Park, H.S. Shin, S.T. Myung, C.S. Yoon, K. Amine, Y.K. Sun, Chem. Mater. 17 (2005) 6–8.
[12] S.B. Jang, S.H. Kang, K. Amine, Y.C. Bae, Y.K. Sun, Electrochim. Acta 50 (2005) 4168–4173.
[13] W. Lu, Z. Chen, H. Joachin, J. Prakash, J. Liu, K. Amine, J. Power Sources 163 (2007) 1074–1079.
[14] Y.S. He, Z.F. Ma, X.Z. Liao, J. Fluorine Chem. 128 (2007) 139–143.
[15] X.F. Luo, X.Y. Wang, L. Liao, S. Gamboa, P.J. Sebastian, J. Power Sources 158 (2006) 654–658.
[16] P. He, H.R. Wang, L. Qi, T. Osaka, J. Power Sources 160 (2006) 627–632.
[17] C.H. Chen, C.J. Wang, B.J. Hwang, J. Power Sources 146 (2005) 626–629.
[18] M.V. Reddy, G.V. Subba Rao, B.V.R. Chowdari, J. Power Sources 159 (2006) 263–267.
[19] A. Van der Ven, D. Morgan, Y.S. Meng, G. Ceder, J. Electrochem. Soc. 153 (2006) A210–A215.
[20] G. Casella, M.R. Guascito, M.G. Sannazzaro, J. Electroanal. Chem. 462 (1999) 202–210.
[21] Y. Zhao, Y.E.L. Fan, Y. Qiu, S. Yang, Electrochim. Acta 52 (2007) 5873–5878.
[22] M. Kang, M.W. Song, C.H. Lee, Appl. Catal. A 251 (2003) 143–156.
[23] L.F. Liotta, G. Di Carlo, G. Pantaleo, A.M. Venezia, G. Deganello, Appl. Catal. B 66 (2006) 217–227.
[24] J.W. Na, J.Y. Kwon, K.S. Han, J. Power Sources 163 (2006) 278–283.
[25] S.H.J. Frank, J. Luminesc. 85 (2000) 193–197.
[26] T. Ohzuku, A. Ueda, M. Nagayama, Y. Iwakoshi, H. Komori, Electrochim. Acta 38 (1993) 1159–1167.
[27] R. Moshtev, P. Zlatilova, V. Manev, K. Tagawa, J. Power Sources 62 (1996) 59–66.
[28] J. Baker, R. Koksbang, M.Y. Saidi, Solid State Ionics 89 (1996) 25–35.